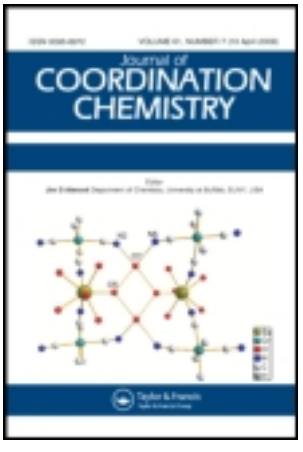

Journal of Coordination Chemistry
Publication details, including instructions for authors and subscription information:
http://www.tandfonline.com/loi/gcoo20

EXAFS study of binuclear hydroxo-bridged copper(II) complexes

Abhijeet Gaur [a], B.D. Shrivastava [a], D.C. Gaur [b], J. Prasad [c], K. Srivastava [c], S.N. Jha [d], D. Bhattacharyya [d], A. Poswal [d] & S.K. Deb [e]

[a] School of Studies in Physics, Vikram University, Ujjain - 452001, India

[b] Physics Department, Government P. G. College, Rajgarh, Biaora - 465661, India

[c] Department of Chemistry, University of Allahabad, Allahabad - 211002, India

[d] Applied Spectroscopy Division, Bhabha Atomic Research Centre, Mumbai - 400085, India

[e] Indus Synchrotron Utilization Division, Raja Ramanna Center for Advanced Technology, Indore - 452013, India

Published online: 08 Apr 2011.

To cite this article: Abhijeet Gaur, B.D. Shrivastava, D.C. Gaur, J. Prasad, K. Srivastava, S.N. Jha, D. Bhattacharyya, A. Poswal & S.K. Deb (2011) EXAFS study of binuclear hydroxo-bridged copper(II) complexes, Journal of Coordination Chemistry, 64:7, 1265-1275

To link to this article: http://dx.doi.org/10.1080/00958972.2011.566604

Journal of Coordination Chemistry
Vol. 64, No. 7, 10 April 2011, 1265–1275

EXAFS study of binuclear hydroxo-bridged copper(II) complexes

ABHIJEET GAUR*†, B.D. SHRIVASTAVA†, D.C. GAUR‡, J. PRASAD§, K. SRIVASTAVA§, S.N. JHA¶, D. BHATTACHARYYA¶, A. POSWAL¶ and S.K. DEB⊥

†School of Studies in Physics, Vikram University, Ujjain – 452001, India
‡Physics Department, Government P. G. College, Rajgarh, Biaora – 465661, India
§Department of Chemistry, University of Allahabad, Allahabad – 211002, India
¶Applied Spectroscopy Division, Bhabha Atomic Research Centre, Mumbai – 400085, India
⊥Indus Synchrotron Utilization Division, Raja Ramanna Center for Advanced Technology, Indore – 452013, India

(*Received 30 September 2010; in final form 24 January 2011*)

Extended X-ray absorption fine structure (EXAFS) measurements have been recorded at the K-edge of copper in binuclear monohydroxo-bridged copper(II) complexes $[(bpy)_2Cu–OH–Cu(bpy)_2](ClO_4)_3$ (**1**) and $[(phen)_2Cu–OH–Cu(phen)_2](C1O_4)_3$ (**2**) and dihydroxo-bridged copper(II) complexes $[Cu_2(\mu–OH)_2(bipy)_2]SO_4 \cdot 5H_2O$ (**3**) and $[Cu_2(\mu–OH)_2(phen)_2]SO_4 \cdot 5H_2O$ (**4**) (where bpy and phen are 2,2′-bipyridine and 1,10-phenanthroline, respectively) using the dispersive EXAFS beamline at 2 GeV Indus-2 synchrotron source at RRCAT, Indore, India. The EXAFS data have been analyzed using the software, *Athena* and *Artemis*. Theoretical models have been generated for **1** and **3** using available crystallographic data and then fitted to their experimental EXAFS data to obtain the structural parameters, which include bond-lengths, coordination numbers, and thermal disorders. The results obtained have been found to be comparable with their crystallographic results. As the crystallographic data for **2** and **4** are not available in the literature, we have determined their structural parameters by fitting their experimental EXAFS data with the same theoretical models which were generated for their corresponding analogous complexes **1** and **3**, respectively. The structural parameters thus determined have been reported. Also, on the basis of the analysis of the EXAFS data, these four complexes have been shown to be binuclear, i.e. they contain two metals. Further, the values of the chemical shifts suggest that copper is in +2 oxidation state in these complexes.

Keywords: Cu(II) complexes; Binuclear; Hydroxo bridged; Cu K-edge EXAFS; Theoretical model

1. Introduction

The study of binuclear complexes of Cu(II) is a very active and highly interesting field due to their significance in bioinorganic chemistry, magnetochemistry, multi-metal catalysis, materials science, superconductivity, and multi-electron redox chemistry [1–3].

*Corresponding author. Email: abhijeetgaur9@gmail.com

Journal of Coordination Chemistry
ISSN 0095-8972 print/ISSN 1029-0389 online © 2011 Taylor & Francis
DOI: 10.1080/00958972.2011.566604

These complexes are also of theoretical interest because they provide examples of the simplest case of magnetic interactions with only two unpaired electrons. These complexes also exhibit ferromagnetic or antiferromagnetic exchange interactions [4]. Binuclear hydroxo-bridged copper(II) complexes have been found [5] to be catalytically active for oxidative coupling reactions, adding to the practical importance of studying the electronic structure of such complexes. Haddad *et al.* [6] reported the preparation and characterization of two binuclear copper(II) complexes bridged by only a single hydroxide, $[(bpy)_2Cu–OH–Cu(bpy)_2](ClO_4)_3$ (**1**) and $[(phen)_2Cu–OH–Cu(phen)_2](ClO_4)_3$ (**2**). They have, however, reported the single-crystal X-ray structure of only **1**, which revealed that it consists of two approximately trigonal bipyramidal Cu(II) centers, with bridging hydroxide occupying an equatorial site on each copper; the remaining sites are filled by the nitrogens of bpy. Srivastava *et al.* [7] also reported electrochemical and spectral studies of **1** and **2**. Similarly, Harris *et al.* [8] reported preparation of two binuclear copper(II) complexes bridged by two hydroxides, $[Cu_2(\mu–OH)_2(bipy)_2]SO_4 \cdot 5H_2O$ (**3**) and $[Cu_2(\mu–OH)_2(phen)_2]SO_4 \cdot 5H_2O$ (**4**) and studied their magnetic moments. Casey *et al.* [9] reported the crystal structure of **3** showing each copper of the dimeric unit is bonded to five donors in a distorted square-pyramidal configuration. The basal atoms are the two bridging oxygens and two nitrogens of a bipyridine. This article reports extended X-ray absorption fine structure (EXAFS) studies of these four hydroxo-bridged complexes.

EXAFS analysis is used to determine the radial distribution of atoms around a particular absorbing atom, thus providing a probe for the structure in the vicinity of the absorbing atom. It gives structural information about the numbers, types, and distances to the neighboring atoms from the absorbing element [10]. EXAFS spectroscopy unambiguously points out whether the given complex is binuclear. If the metal–metal coordination number remains close to unity, it points to the presence of a stable binuclear complex [11]. Study of structurally well-characterized model complexes also provides a benchmark for understanding the EXAFS from metal systems of unknown structure [12]. The significant advantage of X-ray absorption spectroscopy over the X-ray crystallography is that the local structural information around the element of interest can be obtained easily and quickly even from disordered samples, such as powders and solution.

In this study, copper K-edge EXAFS spectra of binuclear monohydroxo-bridged copper(II) complexes **1** and **2** and dihydroxo-bridged copper(II) complexes **3** and **4** have been investigated. The crystallographic data are available for **1** and **3**, from which the theoretical models for these complexes have been generated. These theoretical models are then fitted to their experimental EXAFS data to obtain the structural parameters for **1** and **3** which are comparable with their crystallographic results. The crystallographic data for **2** and **4** are not available in the literature. However, because these two complexes are analogous to **1** and **3**, respectively, we have fitted the same theoretical models, which were generated for **1** and **3**, to the experimental EXAFS data of **2** and **4**, to determine their structural parameters. The structural parameters, thus determined from the EXAFS spectra, for **2** and **4** are reported with the coordination geometries. To our knowledge, EXAFS studies of these hydroxo-bridged complexes have not been made earlier, though, the EXAFS spectra of **2** have been studied by Wong *et al.* [13] and Lee *et al.* [14], but not structural parameters. Only the Fourier transform of the EXAFS spectrum is given and the Cu1–Cu2 distance has been reported as 3.51 Å (uncorrected for phase shift). Also, they have studied this complex only in two MCM-41 mesoporous

forms, tubular (M_T) and particulate (M_P), and their focus was on the difference of EXAFS spectral features between these two forms.

2. Experimental

Complexes **1** and **2** have been prepared by following the methods described by Haddad *et al*. [6] and **3** and **4** by following the methods described by Harris *et al*. [8]. The prepared complexes were characterized by standard chemical methods. The complexes were finely powdered and then absorption screens were prepared by carefully spreading calculated amount of the powder on 1 cm^2 area of kapton tape. The copper K-edge EXAFS spectra of these absorption screens have been recorded at the BL-8 dispersive EXAFS beamline at 2 GeV Indus-2 synchrotron source at Raja Ramanna Center for Advanced Technology (RRCAT), Indore, India [15–17]. The beamline has a 460-mm long Si (1 1 1) crystal having 2-D value equal to 6.2709 Å mounted on an elliptical bender, which can bend the crystal to take shape of an ellipse [18]. The elliptical optics offer minimum aberration. The radiation transmitted through the sample is detected by a position-sensitive CCD detector having 2048×2048 pixels. The whole absorption spectrum can be recorded simultaneously in even a few microseconds for a rich sample. The beamline has a resolution of 1 eV at the photon energies of 10 keV. The plot of absorption *versus* photon energy is obtained by recording the intensities I_0 and I_t, as the CCD outputs, without and with the sample, respectively, and using the relation $I_t = I_0 e^{-\mu x}$, where μ is the absorption coefficient and x is the thickness of the absorber.

For recording the EXAFS spectrum on the dispersive EXAFS beamline, the crystal bender and the goniometer have been set to cover the energy range of the copper K-edge absorption spectra. For energy calibration of that particular setting, absorption spectra at Cu K-edge of Cu metal foil and at Lu L_3-edge of Lu_2O_3 powder have been recorded under the same setting of crystal bender and the goniometer. Taking the values of the energies of Cu K-edge in metal and Lu L_3-edge in Lu_2O_3 as 8980.5 and 9249 eV, respectively [19, 20], the CCD channels have been calibrated.

2.1. *Data analysis*

The EXAFS data of the four complexes have been analyzed using the available computer software packages, *Athena* version 0.8.061 and *Artemis* version 0.8.013 [21] (available from www.xafs.org). These programs include AUTOBK [22] for background removal, FEFF6L [23] for generation of the theoretical EXAFS models, and FEFFIT [24] for parameter optimization of the model. The analysis procedure is as follows.

The spectrum is first normalized by regressing a linear function to the pre-edge region (−200 to −30 eV before the edge energy) and by regressing a linear or quadratic function to the post-edge region (50–1000 eV above the edge energy). Normalized $\mu(E)$ spectra are produced by subtracting the pre-edge line from the entire data spectrum and then dividing the spectrum by the step height [25]. Normalized $\mu(E)$ *versus* E (energy) curves for **1**, **2**, **3**, and **4** are shown in figure 1(a)–(d), respectively. Normalized $\mu(E)$ data are converted to the EXAFS signal $\chi(k)$ data, which are then Fourier transformed. The Fourier transformed data are then fitted with the theoretical model in R-space to obtain

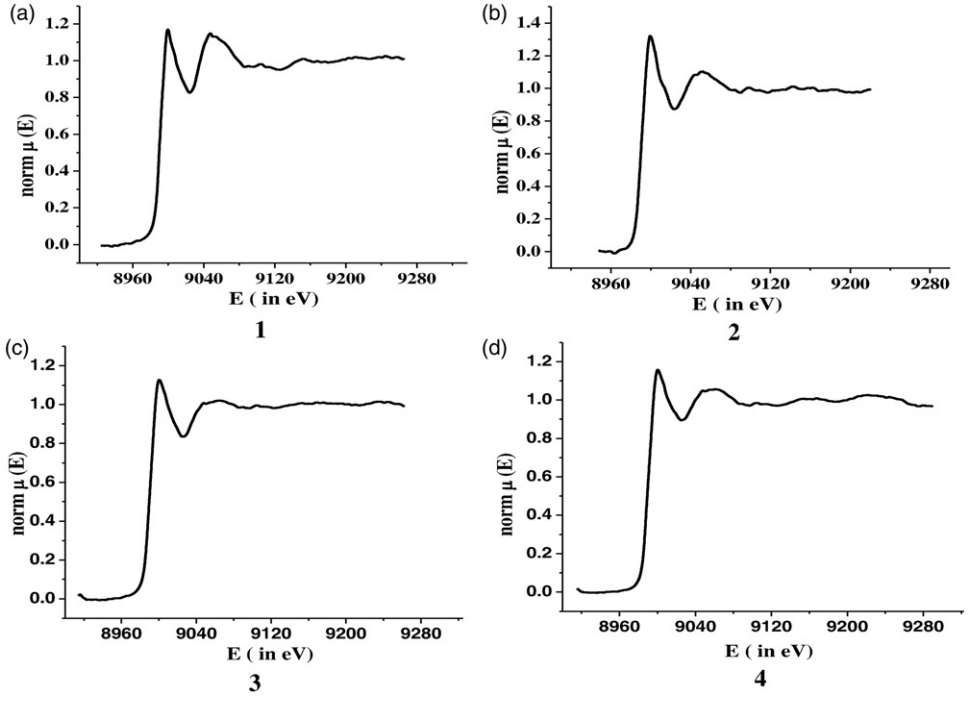

Figure 1. Normalized EXAFS spectra at the K-edge of copper in (a) **1**, (b) **2**, (c) **3**, and (d) **4**.

the different fitting parameters. The theoretical model is written as a sum of paths of the contribution from all scattering paths of photoelectron that travels from the absorbing atom and then is scattered from one or more neighboring atoms and finally returns to the absorbing atom [25–27].

$$\chi(k) \equiv \sum_i [N_i S_0^2 F_{\text{eff}_i}(k)/kR_i^2] \cdot \sin[2kR_i + j_i(k)] \exp(-2\sigma_i^2 k^2) \exp[-2R_i/\lambda(k)], \quad (1)$$

with $R_i = R_{0i} + \Delta R_i$ and

$$k^2 = [2m_e(E - E_0 + \Delta E_0)/\hbar]. \quad (2)$$

In the above equations, the terms $F_{\text{eff}i}(k)$, $\varphi_i(k)$, and $\lambda(k)$ are the effective scattering amplitude, the phase shift, and the mean free path of the photoelectron, respectively, all of which can be calculated by a computer program such as FEFF [28]. The term R_i is the half path length of the photoelectron (i.e. the distance between the absorber and a coordinating atom for a single-scattering event). The value of R_{0i} is the half path length used in the theoretical calculation which can be modified by ΔR_i. Each path has several adjustable parameters optimized by the computer code FEFFIT to fit the data. These parameters include the passive electron-reduction factor (S_0^2), the number of identical paths (N_i), the relative mean-square displacement of the atoms included in path (σ_i^2), an energy shift for each path (ΔE_0), and a change in the path length (ΔR_i).

Table 1. The input positional parameters for **1** (from Haddad *et al.* [6]) and **3** (from Casey *et al.* [9]).

S. No.	Element	*x*	*y*	*z*
1				
1	Cu1	0.23765	0.16054	0.05186
2	Cu2	0.34106	0.22174	−0.1323
3	O1	0.27330	0.16320	−0.0590
4	NA	0.20510	0.26800	0.11070
5	NA′	0.35840	0.19670	0.09530
6	NB	0.11100	0.12860	0.01990
7	NB′	0.20340	0.10910	0.15610
3				
1	Cu1	0.53520	0.42950	0.41580
2	O1	0.42590	0.45920	0.59920
3	O2	0.92620	0.49560	0.66950
4	O3	0.08720	0.39260	0.63790
5	O4	0.81190	0.39040	0.55140
6	N1	0.47050	0.31520	0.40830
7	N2	0.60250	0.39930	0.20290
8	N3	0.94210	0.42750	0.62020

In this study, we have used the following parameters as input in *Artemis* for calculating the theoretical models:

Complex **1**: Space group: $P21/n$,
Cell constants: $a = 14.839$ Å, $b = 18.197$ Å, $c = 16.491$ Å, $\beta = 92.87^\circ$.
Cluster size = 10 Å.
Complex **3**: Space group: $P\bar{1}$,
Cell constants: $a = 7.637$ Å, $b = 16.989$ Å, $c = 8.504$ Å, $\alpha = 91.58^\circ$, $\beta = 97.49^\circ$, $\gamma = 90.36^\circ$.
Cluster size = 10 Å.

The remaining input positional parameters are given in table 1 for complexes **1** and **3**.

The theoretically calculated contributions to $|\chi(R)|$ by the single scattering paths (1) Cu1–O1, (2) four Cu1–N paths, and (3) Cu1–Cu2 path, in **1**, are shown in figure 2(a). Similarly, the theoretically calculated contributions to $|\chi(R)|$ by the single scattering paths (1) three Cu1–O paths, (2) three Cu1–N paths, and (3) Cu1–Cu2 path, in **3**, are shown in figure 2(b). The experimental $|\chi(R)|$ are also shown in these figures.

For generating the theoretical models, we have followed the procedure outlined by Kelly *et al.* [25]. Accordingly, a single value of S_0^2 and ΔE_0 is used for all the paths in the fitting but different values of ΔR can be defined for different paths. Hence, for **1**, out of the four Cu1–N paths, the same ΔR has been defined for the first three paths and another ΔR has been defined for the fourth path. Similarly for **3**, out of the three Cu1–O paths, the same ΔR has been defined for the first two paths and another ΔR for the third path. Also, out of the three Cu1–N paths, the same ΔR has been defined for the first two paths and another ΔR for the third path. Unique Debye–Waller factor (σ^2) values are given to each of the scattering paths in the model. As multiple scattering paths also have important contributions, they have also been included in modeling the data. The resulting fitted curves are shown in figure 3(a) for **1** and 3(c) for **3**. The parameters so obtained are given in table 2 for **1** and table 3 for **3**.

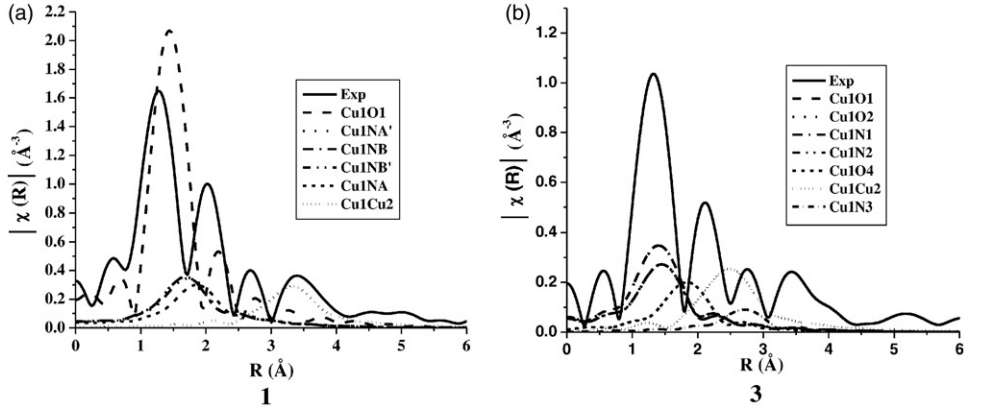

Figure 2. The theoretically calculated contribution to $|\chi(R)|$ by the single scattering paths: Cu1–O1 path, four Cu1–N paths and Cu1–Cu2 path, in **1** (a) and three Cu1–O, three Cu1–N paths and Cu1–Cu2 path, in **3** (b), shown by different dotted/dashed lines given in the inset. The experimental $|\chi(R)|$ of **1** and **3** are shown by solid lines.

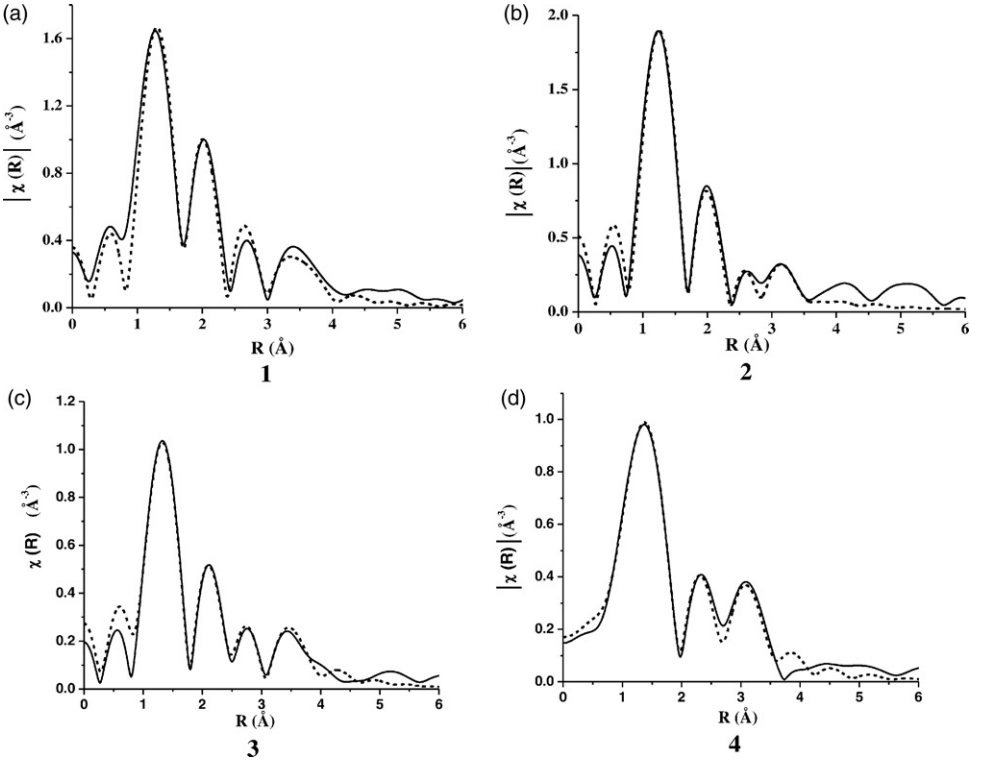

Figure 3. Fourier transformed EXAFS data for (a) **1**, (b) **2**, (c) **3**, and (d) **4**. Solid lines are experimental data and dashed lines are modeled fit as explained in the text.

Table 2. The EXAFS fitting results for **1** and **2**. The XRD results for **1** (from Haddad *et al*. [6]) are also given.

	Complex **1**				Complex **2**			
	EXAFS results				XRD results	EXAFS results		
Atomic pair	N	R (Å)	ΔR (Å)	σ^2 (Å^{-2})	R	N	R (Å)	σ^2 (Å^{-2})
Cu1–O1	1	1.86	−0.06	0.0101 ± 0.0026	1.92	1	1.83	0.0134 ± 0.0017
Cu1–NA′	1	2.18	0.17	0.0123 ± 0.0099	2.00	1	2.09	0.0091 ± 0.0033
Cu1–NB	1	2.18	0.17	0.0123 ± 0.0099	2.01	1	2.10	0.0091 ± 0.0033
Cu1–NB′	1	2.21	0.17	0.0123 ± 0.0099	2.04	1	2.13	0.0091 ± 0.0033
Cu1–NA	1	2.36	0.12	0.0123 ± 0.0099	2.24	1	2.10	0.0091 ± 0.0033
Cu1–Cu2	1	3.60	−0.04	0.0014 ± 0.0049	3.64	1	3.42	0.0087 ± 0.0100

Table 3. The EXAFS fitting results for **3** and **4**. The XRD results for **3** (from Casey *et al*. [9]) are also given.

	Complex **3**				Complex **4**			
	EXAFS results				XRD results	EXAFS results		
Atomic pair	N	R (Å)	ΔR (Å)	σ^2 (Å^{-2})	R	N	R (Å)	σ^2 (Å^{-2})
Cu1–O1	1	1.91	−0.01	0.0082 ± 0.0065	1.92	1	1.86	0.0082 ± 0.0065
Cu1–O2′	1	1.91	−0.01	0.0082 ± 0.0065	1.92	1	1.86	0.0082 ± 0.0065
Cu1–N1	1	1.98	−0.01	0.0082 ± 0.0065	1.99	1	1.94	0.0082 ± 0.0065
Cu1–N2	1	1.99	−0.01	0.0082 ± 0.0065	2.00	1	1.94	0.0082 ± 0.0065
Cu1–O4	1	2.29	−0.09	0.0066 ± 0.0059	2.37	1	2.38	0.0157 ± 0.0063
Cu1–Cu2	1	2.76	−0.08	0.0075 ± 0.0028	2.84	1	2.78	0.0046 ± 0.0022

The theoretical models generated for **1** and **3** have been used to fit the experimental EXAFS data of their analogs **2** and **4**, respectively, to determine their structural parameters. The resulting fitted curves are shown in figure 3(b) for **2** and 3(d) for **4**. The parameters so obtained are given in table 2 for **2** and table 3 for **4**.

3. Results and discussion

The energies of the K-edge of copper are found to be 8989.69, 8990.01, 8988.30, and 8988.11 eV for **1**, **2**, **3**, and **4**, respectively. Taking the energy of copper metal K-edge as 8980.5 eV, the chemical shifts are 9.19, 9.51, 7.80, and 7.61 eV for **1**–**4**, respectively. These values of the chemical shifts suggest that copper is in +2 oxidation state in all four complexes [29, 30].

For analysis of the EXAFS data of **1**, the input parameter, R_{bkg}, that determines the maximum frequency of the background was set to 1.0 Å. Fourier transform was performed over k-range: $k_{\min} = 2.30$ Å^{-1}, $k_{\max} = 8.38$ Å^{-1}. Theoretically modeled data were fitted in the R-space to the experimental data using $k_w = 2$. Fitting was performed for coordination shells in the R ranges of 1.0–5.0 Å. In the fitting procedure, we used the first 16 paths obtained from the FEFF calculations. The value of goodness-of-fit parameter, i.e. reduced chi-square (χ^2_v), is 76.31. The results obtained from fitting are

given in table 2, which gives the local structure parameters for **1** obtained from the analysis. The S_0^2 value obtained is 1.57 with an error of ±0.31. ΔE_0 is also reasonable, i.e. 5.43 eV, with an error of ±1.75. The σ^2 values are quite high as the measurements have been performed at room temperature.

Our results for the bond distances in **1**, with ΔR ranging from −0.04 to 0.17, are given in table 2 and these distances are in agreement with the crystallographic bond distances reported by Haddad *et al.* [6]. The Cu–O bridging distance is 1.86 Å. The axial Cu–N distances are in the range 2.00–2.21 Å. The equatorial distance Cu(1)–NA bond, which is opposite to perchlorate, has a value of 2.36 Å. The Cu(1)–Cu(2) separation is 3.60 Å and the Cu–O–Cu bridging angle calculated from the obtained distances is 150.8°, which is in the range 135.4–165.6° reported for binuclear monohydroxo-bridged complexes [6]; the value of this angle as reported by Haddad *et al.* is 141.6°. Hence, the theoretical model generated by us for **1** appears to be reasonable. Using these results, the inner coordination spheres around the two copper(II) centers are depicted in figure 4(a). This figure is based on the figure given by Haddad *et al.* but shows the distances and bridging angle obtained by us in this study.

For the analysis of the EXAFS data of **3**, the input parameter R_{bkg} was set to 1.1 Å. Fourier transform was performed over k-range: $k_{min} = 2.38\,\text{Å}^{-1}$, $k_{max} = 7.89\,\text{Å}^{-1}$. Theoretically modeled data were fitted in the R-space to the experimental data using $k_w = 2$. Fitting was performed for the coordination shells in the R ranges 1.0–5.0 Å.

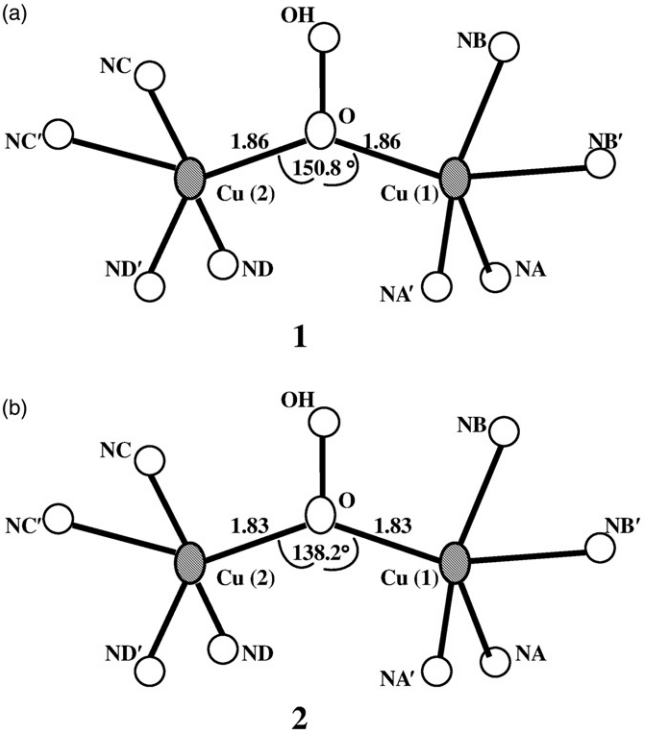

Figure 4. Coordination geometry about copper(II) in **1** (a) and in **2** (b) as deduced from the EXAFS data analysis and following Haddad *et al.* [6].

In the fitting procedure, we used the first 14 paths obtained from the FEFF calculations. The value of reduced chi-square (χ_v^2) is 41.31. The results obtained from fitting are given in table 3, which gives the local structure parameters for **3**. The S_0^2 value obtained is 0.94 with an error of ±0.05. ΔE_0 is also reasonable, i.e. −0.58 eV, with an error of ±1.56. The σ^2 values are quite high for the reason already explained above.

Our results for the bond distances in **3** are in agreement with the crystallographic distances reported by Casey *et al.* [9]. The values of ΔR range from −0.01 to −0.09 and are given in table 3. The four bonds to copper occur in two sets: the average bond-length of copper to two hydroxyl bridged oxygen is 1.91 Å, while copper to bipyridine nitrogen is 1.98 Å. The fifth bond of copper is with sulfate, with Cu–O distance of 2.29 Å. The Cu–Cu separation across the hydroxyl bridges in this complex is 2.76 Å and the Cu–O–Cu bridging angle calculated from the obtained distances comes out to be 91.8°, while the range reported for binuclear dihydroxo-bridged complexes is 95.6–104.1° [31]. The value of this angle as reported by Casey *et al.* is 97.0°. Hence, the theoretical model generated for **3** appears to be quite reasonable. Using the present results the inner coordination spheres around copper(II) centers are depicted in figure 5(a). This figure is based on the figure given by Casey *et al.* but shows the distances and the bridging angle obtained by us in the present study.

As the theoretical model generated by us for **1** fits well to its experimental EXAFS data and as **1** and **2** are analogs, we have used the same theoretical model generated for **1** to fit the experimental EXAFS data of **2**. The data analysis procedure used for **1**, as explained above, has also been applied to **2** and the input fitting parameters were kept the same during fitting. The S_0^2 value obtained is 1.17 with an error of ±0.24. ΔE_0 is also

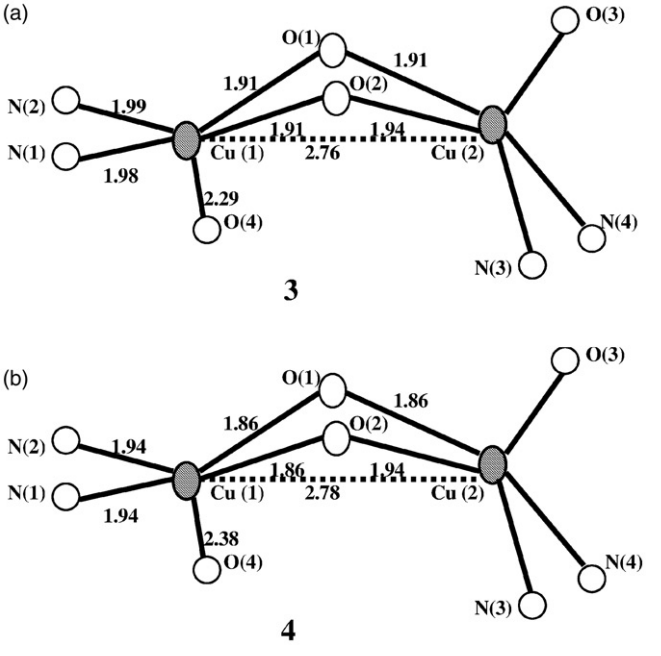

Figure 5. Coordination geometry about copper(II) in **3** (a) and **4** (b) as deduced from the EXAFS data analysis and following Casey *et al.* [9].

reasonable, i.e. −1.25 eV, with an error of ±2.78. The structural parameters so obtained for **2** are reported in table 2. The Cu–O bridging distance is 1.83 Å. The axial Cu–N distances are in the range 2.00–2.14 Å. The equatorial distance Cu(1)–NA bond, which is opposite to the perchlorate site, has a value of 2.10 Å. The Cu(1)–Cu(2) separation is 3.42 Å and the Cu–O–Cu bridging angle calculated from the obtained distances is 138.2°, in the range 135.4–165.6 reported for binuclear monohydroxo-bridged complexes [6]. Using the obtained results, the inner coordination spheres around the two copper(II) centers in **2** are depicted in figure 4(b).

Following the method applied for **1** and **2**, we used the same theoretical model generated for **3** to fit the experimental EXAFS data of its analog **4** following the procedure outlined above. The S_0^2 value obtained is 0.84 with an error of ±0.11. ΔE_0 is also reasonable, i.e. −1.38 eV, with an error of ±4.41. The structural parameters so obtained for **4** are reported in table 3. The four bonds to copper occur in two sets: the copper to hydroxyl bridge oxygen, average 1.86 Å, and the copper to bipyridine nitrogen, average 1.94 Å. The copper has its fifth bond with the sulfate group with a Cu–O distance of 2.38 Å. The Cu–Cu separation across the hydroxyl bridges in this complex (2.78 Å) and the Cu–O–Cu bridging angle calculated from the obtained distances (96.71°) are in the range 95.6–104.1 reported for binuclear dihydroxo-bridged complexes [31]. Using the obtained results, the inner coordination spheres around the copper (II) centers in **4** are depicted in figure 5(b).

Metal–metal coordination numbers in the four complexes are unity (tables 2 and 3), pointing to the presence of a stable binuclear complex [11]. Thus, from the analysis of the EXAFS data, the four complexes have been shown to be binuclear.

4. Conclusions

EXAFS spectra of $[(bpy)_2Cu–OH–Cu(bpy)_2](ClO_4)_3$ (**1**), its analog $[(phen)_2Cu–OH–Cu(phen)_2](C1O_4)_3$ (**2**) and dihydroxo-bridged copper(II) complexes $[Cu_2(\mu–OH)_2(bipy)_2]SO_4 \cdot 5H_2O$ (**3**) and $[Cu_2(\mu–OH)_2(phen)_2]SO_4 \cdot 5H_2O$ (**4**) have been recorded. The EXAFS data have been analyzed and theoretical models have been generated for **1** and **3**, and then fitted to their experimental EXAFS data to obtain the bond-lengths, coordination numbers and thermal disorders. The results obtained from EXAFS data are comparable with the crystallographic results for **1** and **3**. Using the EXAFS results, the inner coordination spheres around the two copper(II) centers in **1** and **3** are pictorially shown.

As the crystallographic data for **2** and **4** are not available in the literature, we have determined the structural parameters for these complexes by fitting their experimental EXAFS data with the same theoretical models generated for their analogs, i.e. **1** and **3**, respectively. The structural parameters, thus determined for **2** and **4** are reported and the inner coordination spheres around the two copper(II) centers in **2** and **4** shown. If crystal structure is available for a complex (which require single crystals), structural parameters like bond-lengths, coordination numbers and Debye–Waller factors can be determined for analogous complexes from EXAFS studies (which do not require single crystals).

The values of the chemical shifts suggest that copper is in +2 oxidation state in all four complexes. Further, on the basis of EXAFS analysis, all the complexes have been shown to be binuclear.

Acknowledgment

The authors thank Madhya Pradesh Council of Science & Technology (MPCST), Bhopal (India) for a research grant.

References

[1] M. Melnik, M. Kabesova, M. Koman, L. Macaskova, J. Garaj, C.E. Holloway, A. Valent. *J. Coord. Chem.*, **45**, 147 (1998).
[2] T.G. Spiro (Ed.). *Copper Proteins*, p. 41, Wiley, New York (1981).
[3] E.I. Soloman, K.W. Penfield, D.E. Wilcox. *Structure and Bonding, Berlin*, **53**, 1 (1983).
[4] Y. Elerman, H. Kara, A. Elmali. *Z. Naturforsch.*, **58a**, 363 (2003).
[5] H.C. Meinders, F. Van Bolhuis, G. Challa. *J. Mol. Catal.*, **5**, 225 (1979).
[6] M.S. Haddad, S.R. Wilson, D.J. Hodgson, D.N. Hendrickson. *J. Am. Chem. Soc.*, **103**, 384 (1981).
[7] K. Srivastava, A.K. Srivastava, J. Prasad. *J. Indian Chem. Soc.*, **86**, 23 (2009).
[8] C.M. Harris, E. Sinn, W.R. Walker, P.R. Woolliams. *Aust. J. Chem.*, **21**, 631 (1968).
[9] A.T. Casey, B.F. Hoskins, F.D. Whillans. *Chem. Commun.*, **708**, 904 (1970).
[10] D.C. Koningsberger, R. Prins (Eds.). *X-ray Absorption: Principles, Applications, Techniques of EXAFS, SEXAFS and XANES*, Wiley, New York (1988).
[11] A.A. Battiston, J.H. Bitter, D.C. Koningsberger. *Catal. Lett.*, **66**, 75 (2000).
[12] J. Yano, V.K. Yachandra. *Photosynth. Res.*, **102**, 241 (2009).
[13] S.-T. Wong, C.-H. Lee, T.-S. Lin, C.-Y. Mou. *J. Catal.*, **228**, 1 (2004).
[14] C.-H. Lee, S.-T. Wong, T.-S. Lin, C.-Y. Mou. *J. Phys. Chem. B*, **109**, 775 (2005).
[15] D. Bhattacharyya, A.K. Poswal, S.N. Jha, Sangeeta, S.C. Sabharwal. *Bull. Mater. Sci.*, **32**, 103 (2009).
[16] D. Bhattacharyya, A.K. Poswal, S.N. Jha, Sangeeta, S.C. Sabharwal. *Nucl. Instrum. Methods A*, **609**, 286 (2009).
[17] N.C. Das, S.N. Jha, D. Bhattacharyya, A.K. Poswal, A.K. Sinha, V.K. Mishra. *Sadhana*, **29**, 545 (2004).
[18] P.L. Lee, M.A. Beno, G. Jennings, M. Ramanathan, G.S. Knapp, K. Huang, J. Bai, P.A. Montano. *Rev. Sci. Instrum.*, **65**, 1 (1994).
[19] J.A. Bearden, *X-ray Wavelengths*, pp. 456, 468, US Atomic Energy Commission, Oak Ridge, TN (1964).
[20] R.D. Deslattes, E.G. Kessler Jr, P. Indelicato, L. de Billy, E. Lindroth, J. Anton. *Rev. Mod. Phys.*, **75**, 35 (2003).
[21] B. Ravel, M. Newville. *J. Synchrotron Radiat.*, **12**, 537 (2005).
[22] M. Newille, P. Livins, Y. Yacoby, J.J. Rehr, E.A. Stern. *Phys. Rev. B*, **47**, 14126 (1993).
[23] S.I. Zabinsky, J.J. Rehr, A. Ankudinov, R.C. Albers, M.J. Eller. *Phys. Rev. B*, **52**, 2995 (1995).
[24] M. Newville, B. Ravel, D. Haskel, J.J. Rehr, E.A. Stern, Y. Yacoby. *Physica B*, **208–209**, 154 (1995).
[25] S.D. Kelly, D. Hesterberg, B. Ravel. *Methods of Soil Analysis, Part 5, Mineralogical Methods*, pp. 387–463, Soil Science Society of America, Madison, WI (2008).
[26] E.A. Stern. *Contemp. Phys.*, **19**, 239 (1978).
[27] E.A. Stern, S.M. Heald. In *Handbook of Synchrotron Radiation*, E.E. Koch (Ed.), Vol. 10, p. 995, Amsterdam, North Holland (1983).
[28] J.J. Rehr, R.C. Albers. *Rev. Mod. Phys.*, **72**, 621 (2000).
[29] L.S. Kau, D.J. Spira-Solomon, J.E. Penner-Hahn, K.O. Hodgson, E.I. Solomon. *J. Am. Chem. Soc.*, **109**, 6433 (1987).
[30] J.L. Fulton, M.M. Hoffman, J.G. Darab, B.J. Palmer, E.A. Stern. *J. Phys. Chem. A*, **104**, 11651 (2000).
[31] V.H. Crawford, H.W. Richardson, J.R. Wasson, D.J. Hodgson, W.E. Hatfield. *Inorg. Chem.*, **15**, 2107 (1976).